Bell Correlations in Spin-Squeezed States of 500 000 Atoms

Nils J. Engelsen, Rajiv Krishnakumar, Onur Hosten, and Mark A. Kasevich*
Department of Physics, Stanford University, Stanford, California 94305, USA
(Received 23 November 2016; published 3 April 2017)

Bell correlations, indicating nonlocality in composite quantum systems, were until recently only seen in small systems. Here, we demonstrate Bell correlations in squeezed states of 5×10^5 ^{87}Rb atoms. The correlations are inferred using collective measurements as witnesses and are statistically significant to 124 standard deviations. The states are both generated and characterized using optical-cavity aided measurements.

DOI: 10.1103/PhysRevLett.118.140401

Progress in the control of quantum systems has been accompanied by the development of metrics quantifying quantum correlations in many-body systems [1–4]. A widely adopted measure for systems with large numbers of particles is the depth of entanglement [5–7]. This measure characterizes the minimal number of particles that are mutually entangled in a system. However, not all types of quantum correlations can be classified using the concept of entanglement alone [8,9]. An example is the Bell-type correlations which are exhibited by quantum systems violating Bell's inequalities [10].

Demonstrating nonlocal Bell correlations was restricted to small systems in which the individual components of a composite quantum system can be measured directly. Bell correlations have been shown with photons [11–14], ions [15], atoms [16], solid-state spins [17], and nitrogen-vacancy centers [18]. To extend the investigation of Bell correlations to larger systems, a new framework was developed in Ref. [19] that enables observation of Bell correlations without accessing individual components of a system. This framework provides a method to witness whether a quantum many-body system features nonlocality, as evidenced by Bell correlations. The method was employed in Ref. [20] with measurements that access only the collective observables of a Bose-Einstein condensate of 480 ^{87}Rb atoms to demonstrate Bell correlations with a statistical significance of 3.8 standard deviations. In this Letter, we show Bell correlations in spin-squeezed states in a thermal ensemble of 5×10^5 ^{87}Rb atoms at 25 μK which are statistically significant to 124 standard deviations. While our result demonstrates the presence of Bell correlations, it cannot be used to perform loophole-free tests of Bell's inequalities, as the measurement duration is longer than the time of flight for light across the sample (the no-communication loophole [8]), and the Bell correlation witness [Eq. (2)] *a priori* assumes quantum mechanics in its derivation [20].

We describe our atomic ensemble as a system of N spin-1/2 particles. Experimentally, we utilize the clock states of ^{87}Rb and define $|F=2,m_F=0\rangle\equiv|\uparrow\rangle$ and $|F=1,m_F=0\rangle\equiv|\downarrow\rangle$ as our pseudospin states. For a measurement of the ith spin on a given axis $\mathbf{m}$, only two measurement outcomes are possible, $j_{\mathbf{m}}^{(i)}=\pm1/2$. Considering two possible axis choices, defined by the unit vectors $\mathbf{m}$ and $\mathbf{n}$, the quantities relevant for constructing a Bell inequality are the expectation values $\langle j_{\mathbf{m}}^{(i)}\rangle$ and the correlations $\langle j_{\mathbf{m}}^{(i)}j_{\mathbf{m}}^{(k)}\rangle$, $\langle j_{\mathbf{m}}^{(i)}j_{\mathbf{n}}^{(k)}\rangle$, $\langle j_{\mathbf{n}}^{(i)}j_{\mathbf{n}}^{(k)}\rangle$. Simple algebraic combinations of these one- and two-body correlators, such as $\mathcal{S}_{\mathbf{m}}=2\sum_{i=1}^{N}\langle j_{\mathbf{m}}^{(i)}\rangle$ and $\mathcal{S}_{\mathbf{mn}}=4\sum_{i,k=1,i\neq k}^{N}\langle j_{\mathbf{m}}^{(i)}j_{\mathbf{n}}^{(k)}\rangle$, lead to a Bell inequality under the assumption of permutation symmetry of the spins in the system [19]:

$$2\mathcal{S}_{\mathbf{m}}+\mathcal{S}_{\mathbf{mm}}/2+\mathcal{S}_{\mathbf{mn}}+\mathcal{S}_{\mathbf{nn}}/2+2N\geq0. \tag{1}$$

This Bell inequality can be used to derive a Bell correlation witness requiring measurements of only the collective spin vector $\mathbf{J}\equiv\sum_{i=1}^{N}\mathbf{j}^{(i)}$, where $\mathbf{j}^{(i)}=(j_x^{(i)},j_y^{(i)},j_z^{(i)})$. The presence of Bell correlations can then be probed with measurements of these collective observables alone [20,21]. This is analogous to the widely adopted entanglement depth measure for characterizing entanglement in systems with large numbers of particles [5–7], which makes an inference on the size of entangled clusters from measurements of collective observables. Note that these kinds of inferences require repeated observations of identically prepared states of the system.

A particular class of collective states that can violate Eq. (1) are spin-squeezed states [22]. For a symmetric collective state of N spins, assuming a mean polarization along the x direction, the uncertainty of two orthogonal components of $\mathbf{J}$ is limited by the relation $\Delta J_{\mathbf{z}}\,\Delta J_{\mathbf{y}}\geq N/4$. Spins that are each independently polarized along the x direction comprise a coherent spin state (CSS), an unentangled minimum uncertainty state where $\Delta J_{\mathbf{z}}=\Delta J_{\mathbf{y}}=\sqrt{N}/2$ defines the CSS noise. Spin squeezing redistributes the uncertainty from one conjugate variable to the other, generating entanglement between the spins in the process. As a consequence of the uncertainty principle, reduction in uncertainty in one conjugate variable (squeezing) comes at the expense of a corresponding increase in the uncertainty

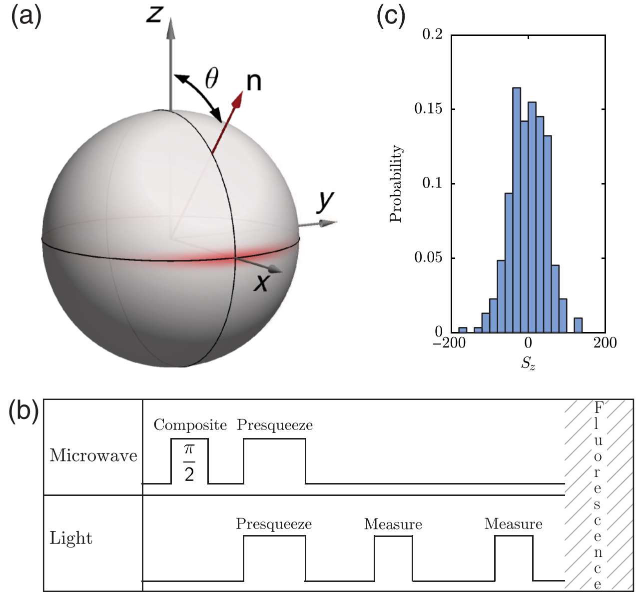

FIG. 1. (a) Illustration of a squeezed spin state. The example is a Wigner distribution of a 10 dB squeezed state with 30 atoms, polarized along the x axis. Squeezing is along the z direction, while antisqueezing is along the y direction. Also shown is the axis $\mathbf{n}$ used to calculate the Bell witness in Eq. (2). (b) The sequence used for squeezing. The initial state preparation consists of a composite $\pi/2$ pulse and a presqueezing procedure that squeezes the state in $S_\mathbf{z}$ such that the initial uncertainty is smaller than the cavity linewidth. The two QND measurements then follow, before a final fluorescence measurement that measures the atom number. (c) Histogram of the differences in S_z between the first and second measurements for 18.5(3) dB squeezed states of 6.5×10^5 atoms.

for the other conjugate variable (antisqueezing). For sufficient amounts of squeezing, the squeezed states may also contain Bell correlations.

Choosing a specific set of measurement axes determined by two unit vectors $\mathbf{z}$ and $\mathbf{n}$ [Fig. 1(a)], the witness function can be expressed in terms of the expectation values of the normalized collective spin operators $\mathcal{J}_{1,\mathbf{n}} \equiv \langle 2J_\mathbf{n}/N \rangle$ and $\mathcal{J}_{2,\mathbf{z}} \equiv \langle 4J_\mathbf{z}^2/N \rangle$, where $J_\mathbf{z} \equiv \mathbf{z} \cdot \mathbf{J}$ and $J_\mathbf{n} \equiv \mathbf{n} \cdot \mathbf{J}$. The witness inequality then reads [20]

$$\langle W \rangle = -|\mathcal{J}_{1,\mathbf{n}}| + (\mathbf{z} \cdot \mathbf{n})^2 \mathcal{J}_{2,\mathbf{z}} + 1 - (\mathbf{z} \cdot \mathbf{n})^2 \geq 0. \quad (2)$$

In this expression, the total particle number N inside the expectation values is allowed to be a fluctuating random variable, which in our experiment has a 3% standard deviation from one realization to the next. The first term can be measured by rotating the collective spin state, which amounts to changing the angle between $\mathbf{z}$ and $\mathbf{n}$. $\mathcal{J}_{1,\mathbf{n}}$ can then be found by measuring the projection of the state on the z direction after the rotation. The second term, where $\langle J_z \rangle = 0$, is simply proportional to the variance of $J_\mathbf{z}$ normalized to the CSS noise. Equation (2) is the first criterion that we will use to demonstrate Bell correlations. From Eq. (2), it follows that the inequality

$$\mathcal{J}_{2,\mathbf{z}} < \frac{1}{2}[1 - (1 - \mathcal{J}_{1,\mathbf{x}}^2)^{1/2}] \quad (3)$$

also guarantees Bell correlations (a full derivation can be found in the Supplemental Material of Ref. [20]). Here, assuming a squeezed state with $\langle J_z \rangle = 0$, the quantity $\mathcal{J}_{1,\mathbf{x}}$ is simply the coherence of the state. This second criterion is more robust to experimental noise, and it is with this criterion that we get the most statistically significant violation. Similarly to the entanglement depth criterion, the Bell violation witness function is fully parametrized by the coherence (the length of the Bloch vector) and the amount of squeezing in the state [5,6].

The experimental apparatus and preparation of the squeezed states is described in Ref. [23]. We trap up to 7×10^5 cold atoms in an optical lattice generated by 1560 nm light inside of an optical cavity. The cavity mirrors are coated to support both 780 and 1560 nm modes. A 780 nm mode is used to perform quantum nondemolition (QND) measurements of the collective state of the atoms to prepare the squeezed states. We set the detuning between the atomic resonance and the 780 nm cavity mode such that the effect of the atoms is a state-dependent change in the refractive index—equal in magnitude but opposite in sign for the $|\uparrow\rangle$ and $|\downarrow\rangle$ states. The refractive index change then manifests as a cavity resonance shift, whose measurement serves as a QND measurement of $J_\mathbf{z}$. The technical noise limit of this QND measurement is 41 dB below the CSS noise limit, which means the QND measurement of J_z is limited only by the quantum noise [23].

For the purposes of showing Bell correlations, we seek to measure the symmetric collective observable $J_\mathbf{z} = \sum_{i=1}^N j_z^{(i)}$. A cavity where each atom is identically coupled to the probe mode would measure this observable. In this experiment, the 1560 nm light traps the atoms at the peaks of the 780 nm standing wave intensity profile, enabling uniform coupling of the atoms to the probe. However, there is still some residual inhomogeneity due to the finite temperature of the atoms and the finite size of the cloud, which extends over ~1000 lattice sites (780 μm) along the cavity axis. We can therefore measure only the collective observable $S_\mathbf{z} = (1/Z) \sum_{i=1}^N (1 - \epsilon_i) j_z^{(i)}$, where Z is a normalization constant and ϵ_i is a small quantity parametrizing the reduction from unity in the coupling of atom i. In our setup, we have measured a $\sim 5 \times 10^{-3}$ fractional variance in the atom-probe coupling (see Ref. [23] for details on the measurement of the atom-cavity coupling). This determines the deviation from symmetry in the measurement of the collective spin observables.

To generate squeezing in our apparatus, the atoms, initially prepared in the $|\downarrow\rangle$ state, are put in an equal superposition of the $|\uparrow\rangle$ and $|\downarrow\rangle$ states using a microwave drive [Fig. 1(b)]. Two QND measurements are then performed. The first measurement projects the collective spin state into one with reduced $S_\mathbf{z}$ uncertainty and increased $S_{\mathbf{y}}$ uncertainty. The second measurement verifies the squeezing by showing better correlation with the first measurement than is allowed with unentangled states. Using this method we generate and characterize up to 20 dB of spin squeezing by the Wineland criterion $[|\langle S_x\rangle|/(\sqrt{N}\Delta S_z)]^2$ [24]. Following the first measurement generating the squeezing, we can choose to drive Rabi oscillations using microwaves, amounting to a rotation of the collective spin state about the y axis. This way, a subsequent measurement of $S_{\mathbf{z}}$ allows us to determine $S_{\mathbf{n}}$ for any chosen angle θ between $\mathbf{z}$ and $\mathbf{n}$. Since the squeezing is conditional on the outcome of the QND measurement, the inferred $\langle S_z\rangle$ for the prepared squeezed states is different in each realization. In order to show the Bell correlations, we therefore choose an axis $\mathbf{z}'$ at each realization such that the inferred $\langle S_{\mathbf{z}'}\rangle = 0$. The shot-to-shot variation in the chosen axis can be accounted for as noise in θ in Eq. (2) (see the Supplemental Material [25]). For our parameters, this noise is small compared to the noise added by microwave rotation noise.

To relate the measured $S_{\mathbf{z}}$ observable to the properties of $J_{\mathbf{z}}$, we use a conservative procedure based on a model that was verified experimentally [23]. In this model, ϵ_i depends on the specific position of the atom and is randomized in each experimental run. The randomization of the position can be modeled as an additive noise that would appear in a measurement of the uniform observable $J_{\mathbf{z}}$. In our setup, this additive noise is 16.8(7) dB below the CSS noise [23]. The error on this quantity is estimated from the additive noises found at three different atom numbers. According to this model, the squeezed state shown in Fig. 1(c), for example, which is 18.5 dB squeezed in $S_{\mathbf{z}}$, is guaranteed to be squeezed by at least 14.5 dB in $J_{\mathbf{z}}$. For all Bell correlation data presented below, we calculate $\mathcal{J}_{2,\mathbf{z}}$ according to this model. The error on this quantity is obtained by adding in quadrature the error in the squeezing measurements and the error from the J_z estimation model.

While we measure the squeezing levels using the cavity probe, the Rabi oscillations needed to determine $\mathcal{J}_{1,\mathbf{n}}$ are characterized using fluorescence imaging since the cavity does not have the dynamic range to make these measurements. The fluorescence imaging is done by first releasing the atoms from the optical lattice, then pushing the atoms in the $|\uparrow\rangle$ state with a laser resonant with the $|F=2\rangle \rightarrow |F'=3\rangle$ transition. After a 1.2 ms time of flight, the spatially separated states are imaged for 2 ms with resonance fluorescence. The signal from the pushed $|\uparrow\rangle$ atoms is 20% lower due to lower fluorescence beam intensity at their location. We performed a calibration to correct for this and applied it to the raw data. The error in the calibration procedure is insignificant compared to the statistical errors for the presented data.

For a data set containing 15.0(7) dB inferred squeezing in J_z, we plot the observed Rabi oscillations in Fig. 2. Combining the Rabi oscillation data with the squeezing

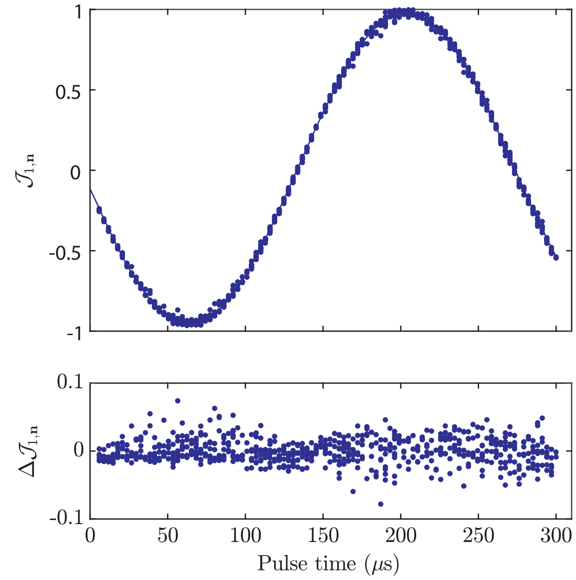

FIG. 2. Rabi oscillations of squeezed states of 6.5×10^5 atoms. (Upper panel) $\mathcal{J}_{1,\mathbf{n}}$ as a function of the microwave pulse time. The fit is sinusoidal and is used to extract the angle for the witness function in Fig. 3. The fit shows a contrast of 94.9(1)%. (Lower panel) Residuals from subtracting the sine fit from the data points. The increased noise at the $\mathcal{J}_{1,\mathbf{n}} \approx \pm 1$ points is due to antisqueezing. Fluorescence detection noise dominates at short pulse times, while microwave amplitude noise takes over at longer pulse times. Pulse times below 5 μs were not achievable due to control system limitations.

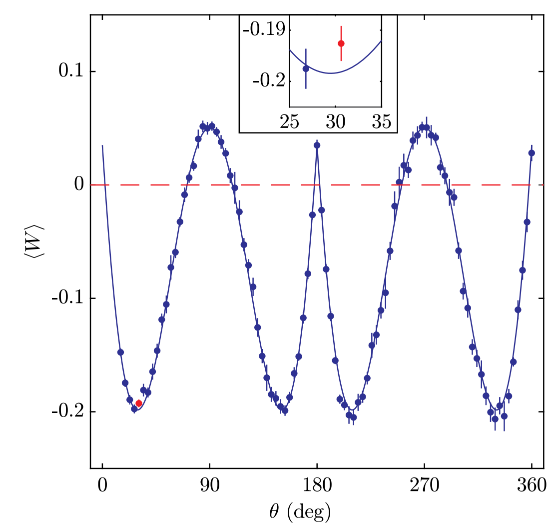

FIG. 3. The data points show the Bell correlation witness $\langle W\rangle$ as a function of θ. The θ values are extracted from the fit in Fig. 2. The error bars show the combined statistical error from the measured $\mathcal{J}_{1,\mathbf{n}}$ and the total error in the estimated $\mathcal{J}_{2,\mathbf{z}}$ value. Points below the dashed red line show a violation of the inequality in Eq. (2). The highest violation is from the point shown in red (and also in the inset) which is 56 standard deviations from the boundary. The solid blue line is calculated from the contrast of the fit to the Rabi fringe and the squeezing level. For a maximally squeezed state with 100% coherence, the minimum of the witness function would approach −0.25.

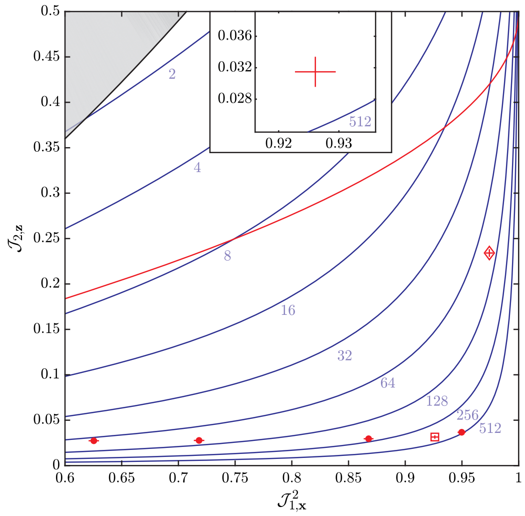

FIG. 4. Entanglement depth and Bell correlation boundaries. The red line shows the Bell violation boundary according to Eq. (3). The blue lines show the boundary for $k = 2^n$ entanglement depth for $n = 1, \ldots, 9$ (labeled below each line). The area below the black line contains entangled states according to the Wineland criterion for entanglement [30]. The data points, taken with 5×10^5 atoms and approximately 450 measurements each, have measurement strengths going from higher on the left to lower on the right. The error bars represent 68% confidence intervals. The open-square data point shows the most statistically significant demonstration of Bell correlations (the inset is an enlarged version of this data point). The open-diamond data point shows the result from a data set of 3286 runs with unconditional squeezing.

level, we plot the witness function $\langle W \rangle$ in Fig. 3. All data points below the dashed line indicate nonlocal correlations in the prepared squeezed states. The dominant contribution to the error bars is the noise of the microwave rotation, which amounts to an uncertainty in the angle θ between $\mathbf{z}$ and $\mathbf{n}$. This leads to increasing uncertainties with an increasing microwave drive time.

In Fig. 4 we plot our data with the Bell correlation boundary and entanglement depth boundaries on the $\mathcal{J}^2_{1,\mathbf{x}} - \mathcal{J}_{2,\mathbf{z}}$ plane. Here, the $\mathcal{J}_{1,\mathbf{x}}$ values of the states were determined by first performing the squeezing measurement, then making a microwave $\pi/2$ rotation about the y axis to turn $J_\mathbf{x}$ into $J_\mathbf{z}$. The observable $J_\mathbf{z}$ was then measured using fluorescence imaging in 200 repetitions. For error estimation, the fluorescence calibration errors as well as the statistical errors are taken into account. In Fig. 4, we also show a data set that was unconditionally squeezed by 8.5 dB. These states were prepared using a similar method to that in Ref. [28]. The best conditionally squeezed data is 124 standard deviations from the boundary; the corresponding number for unconditional squeezing is 33 (see the Supplemental Material [25] for details). The largest entanglement depth obtained in this analysis is approximately 500. However, using a more optimal entanglement depth criterion tailored for nonsymmetric probing [29], the best entanglement depth becomes 1590(130) [25].

In Ref. [20], it was shown that there exist non-Gaussian states that do not contain Bell correlations, but that nevertheless violate the witness inequalities in Eqs. (2) and (3). These non-Gaussian states can only be ruled out by performing $\sim N$ measurements. As there exists no known mechanism to generate these non-Gaussian states in our experiment, here we have assumed that the generated squeezed states are Gaussian states.

In conclusion, we have shown statistically significant Bell correlations in a large, thermal ensemble of ^{87}Rb atoms. Bell correlations measure nonlocality, which can be used as a resource in quantum information. While the use of Bell correlations in many-body systems is still unknown, they have been used to generate random numbers in smaller systems [31]. Recent experiments have shown large spatial separation of quantum superpositions of atomic wave packets [32]. Combining the ideas of spin squeezing with spatially separated superpositions, the Bell correlations discussed in this Letter could perhaps be used to test quantum mechanics in new ways.

We would like to thank Remigiusz Augusiak, Luca Dellantonio, and Jaya Krishnakumar for the fruitful discussions. This work was supported by the Office of Naval Research, the Defense Threat Reduction Agency and the Vannevar Bush Faculty Fellowship program.

*kasevich@stanford.edu

[1] R. Horodecki, P. Horodecki, M. Horodecki, and K. Horodecki, Quantum entanglement, Rev. Mod. Phys. **81**, 865 (2009).

[2] N. Li and S. Luo, Entanglement detection via quantum Fisher information, Phys. Rev. A **88**, 014301 (2013).

[3] C. W. Helstrom, Minimum mean-squared error of estimates in quantum statistics, Phys. Lett. **25A**, 101 (1967).

[4] S. L. Braunstein and C. M. Caves, Statistical Distance and the Geometry of Quantum States, Phys. Rev. Lett. **72**, 3439 (1994).

[5] A. S. Sørensen and K. Mølmer, Entanglement and Extreme Spin Squeezing, Phys. Rev. Lett. **86**, 4431 (2001).

[6] B. Lücke, J. Peise, G. Vitagliano, J. Arlt, L. Santos, G. Tóth, and C. Klempt, Detecting Multiparticle Entanglement of Dicke States, Phys. Rev. Lett. **112**, 155304 (2014).

[7] S. B. Papp, K. S. Choi, H. Deng, P. Lougovski, S. J. van Enk, and H. J. Kimble, Characterization of multipartite entanglement for one photon shared among four optical modes, Science **324**, 764 (2009).

[8] N. Brunner, D. Cavalcanti, S. Pironio, V. Scarani, and S. Wehner, Bell nonlocality, Rev. Mod. Phys. **86**, 419 (2014).

[9] A set of examples is displayed in the Werner states, which are mixed states defined by the density matrix $\rho = p|\phi_+\rangle\langle\phi_+| + (1-p)I/4$. Here, $|\phi_+\rangle = (1/\sqrt{2})(|\uparrow\uparrow\rangle + |\downarrow\downarrow\rangle)$ is a Bell state and the identity matrix I represents a maximally mixed state. For $1/3 < p < 1/2$, these states are entangled but do not violate any Bell inequalities.

[10] J. F. Clauser, M. A. Horne, A. Shimony, and R. A. Holt, Proposed Experiment to Test Local Hidden-Variable Theories, Phys. Rev. Lett. **23**, 880 (1969).
[11] M. Eibl, S. Gaertner, M. Bourennane, C. Kurtsiefer, M. Żukowski, and H. Weinfurter, Experimental Observation of Four-Photon Entanglement from Parametric Down-Conversion, Phys. Rev. Lett. **90**, 200403 (2003).
[12] Z. Zhao, T. Yang, Y.-A. Chen, A.-N. Zhang, M. Żukowski, and J. W. Pan, Experimental Violation of Local Realism by Four-Photon Greenberger-Horne-Zeilinger Entanglement, Phys. Rev. Lett. **91**, 180401 (2003).
[13] M. Giustina *et al.*, Significant-Loophole-Free Test of Bell's Theorem with Entangled Photons, Phys. Rev. Lett. **115**, 250401 (2015).
[14] L. K. Shalm *et al.*, Strong Loophole-Free Test of Local Realism, Phys. Rev. Lett. **115**, 250402 (2015).
[15] B. P. Lanyon, M. Zwerger, P. Jurcevic, C. Hempel, W. Dür, H. J. Briegel, R. Blatt, and C. F. Roos, Experimental Violation of Multipartite Bell Inequalities with Trapped Ions, Phys. Rev. Lett. **112**, 100403 (2014).
[16] J. Hofmann, M. Krug, N. Ortegel, L. Gérard, M. Weber, W. Rosenfeld, and H. Weinfurter, Heralded entanglement between widely separated atoms, Science **337**, 72 (2012).
[17] W. Pfaff, T. H. Taminiau, L. Robledo, H. Bernien, M. Markham, D. J. Twitchen, and R. Hanson, Demonstration of entanglement-by-measurement of solid-state qubits, Nat. Phys. **9**, 29 (2013).
[18] B. Hensen, H. Bernien, A. E. Dréau, A. Reiserer, N. Kalb, M. S. Blok, J. Ruitenberg, R. F. L. Vermeulen, R. N. Schouten, C. Abellán, W. Amaya, V. Pruneri, M. W. Mitchell, M. Markham, D. J. Twitchen, D. Elkouss, S. Wehner, T. H. Taminiau, and R. Hanson, Loophole-free Bell inequality violation using electron spins separated by 1.3 kilometres, Nature (London) **526**, 682 (2015).
[19] J. Tura, R. Augusiak, A. B. Sainz, T. Vértesi, M. Lewenstein, and A. Acín, Detecting nonlocality in many-body quantum states, Science **344**, 1256 (2014).
[20] R. Schmied, J.-D. Bancal, B. Allard, M. Fadel, V. Scarani, P. Treutlein, and N. Sangouard, Bell correlations in a Bose-Einstein condensate, Science **352**, 441 (2016).
[21] J. Tura, R. Augusiak, A. B. Sainz, B. Lücke, C. Klempt, M. Lewenstein, and A. Acín, Nonlocality in many-body quantum systems detected with two-body correlators, Ann. Phys. (Berlin) **362**, 370 (2015).
[22] M. Kitagawa and M. Ueda, Squeezed spin states, Phys. Rev. A **47**, 5138 (1993).
[23] O. Hosten, N. J. Engelsen, R. Krishnakumar, and M. A. Kasevich, Measurement noise 100 times lower than the quantum-projection limit using entangled atoms, Nature (London) **529**, 505 (2016).
[24] D. J. Wineland, J. J. Bollinger, W. M. Itano, and D. J. Heinzen, Squeezed atomic states and projection noise in spectroscopy, Phys. Rev. A **50**, 67 (1994).
[25] See Supplemental Material at http://link.aps.org/supplemental/10.1103/PhysRevLett.118.140401 for further details on conditional squeezing, the nonsymmetric entanglement criterion, the calculation of statistical significance, which includes Refs. [26,27].
[26] G. Vitagliano, I. Apellaniz, M. Kleinmann, B. Lücke, C. Klempt, and G. Toth, Entanglement and extreme spin squeezing of unpolarized states, New J. Phys. **19**, 013027 (2017).
[27] L. Dellantonio, master's thesis, University of Copenhagen, 2015.
[28] O. Hosten, R. Krishnakumar, N. J. Engelsen, and M. A. Kasevich, Quantum phase magnification, Science **352**, 1552 (2016).
[29] L. Dellantonio, S. Das, J. Appel, and A. S. Sørensen, Multipartite entanglement detection with non symmetric probing, arXiv:1609.08516.
[30] A. Sørensen, L.-M. Duan, J. I. Cirac, and P. Zoller, Many-particle entanglement with Bose–Einstein condensates, Nature (London) **409**, 63 (2001).
[31] S. Pironio, A. Acín, S. Massar, A. Boyer de la Giroday, D. N. Matsukevich, P. Maunz, S. Olmschenk, D. Hayes, L. Luo, T. A. Manning, and C. Monroe, Random numbers certified by Bell's theorem, Nature (London) **464**, 1021 (2010).
[32] T. Kovachy, P. Asenbaum, C. Overstreet, C. A. Donnelly, S. M. Dickerson, A. Sugarbaker, J. M. Hogan, and M. A. Kasevich, Quantum superposition at the half-metre scale, Nature (London) **528**, 530 (2015).